

Numerical Modeling of Jellyfish Galaxy at Intel Xeon Phi supercomputers

**Igor Kulikov, Igor Chernykh, Victor Protasov
ICM&MG SB RAS**

**1 December 2017
Moscow, Russia**

The general problem: AGN is the driver of ram-pressure?



Poggianti B., Jaffé Y., Moretti A. et al. Ram-pressure feeding of supermassive black holes // Nature. – 2017. – V. 548. – P. 304-309

The motivation – (i) physics

«The movement of galaxies in dense clusters turns the collisions of galaxies into an important evolutionary factor»

***Professor
Alexander Tutukov***



The motivation and challenges for me are:

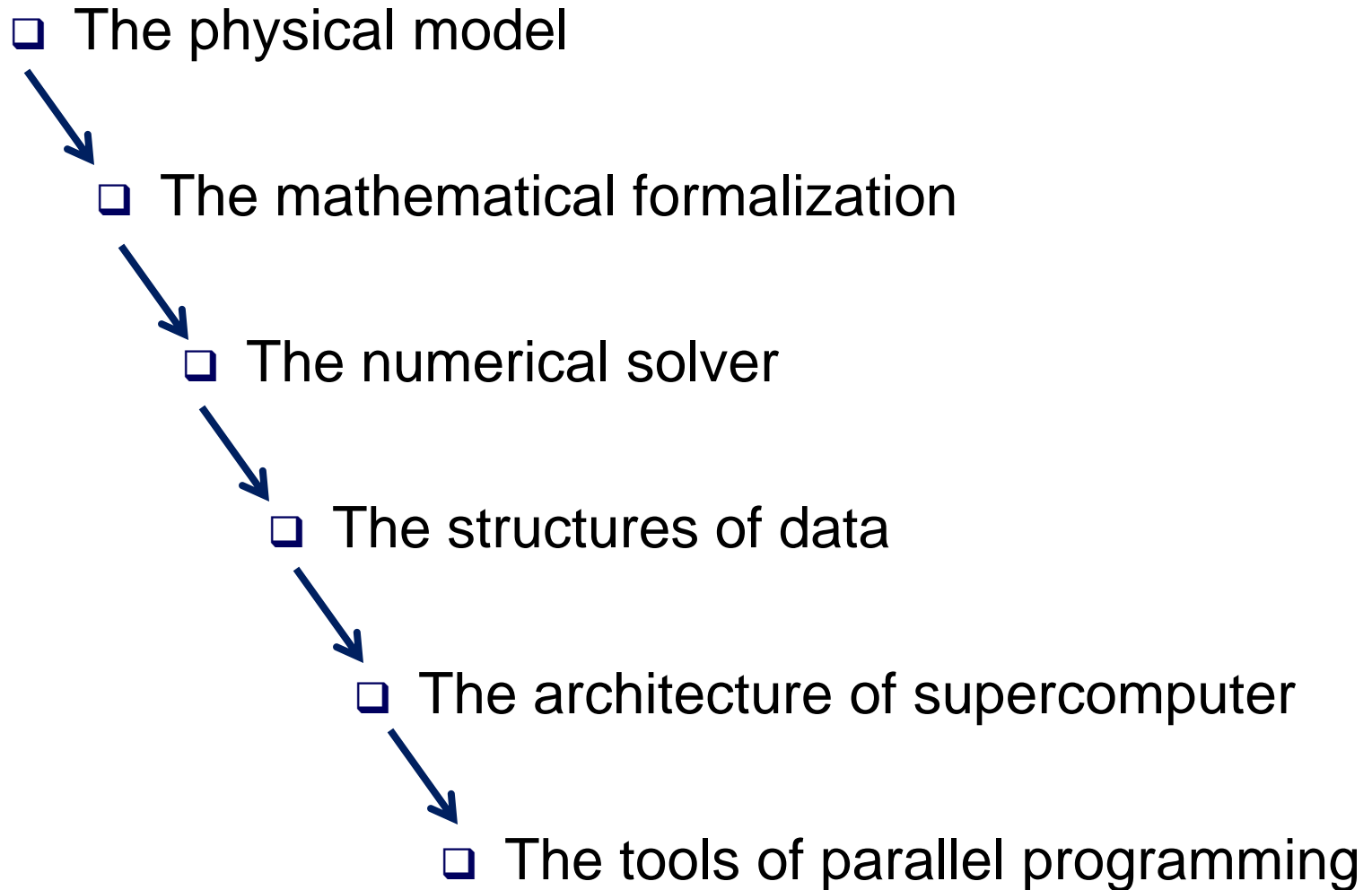
1. The model of galaxy
2. The numerical solver
3. The parallel implementation

The motivation – (ii) supercomputers

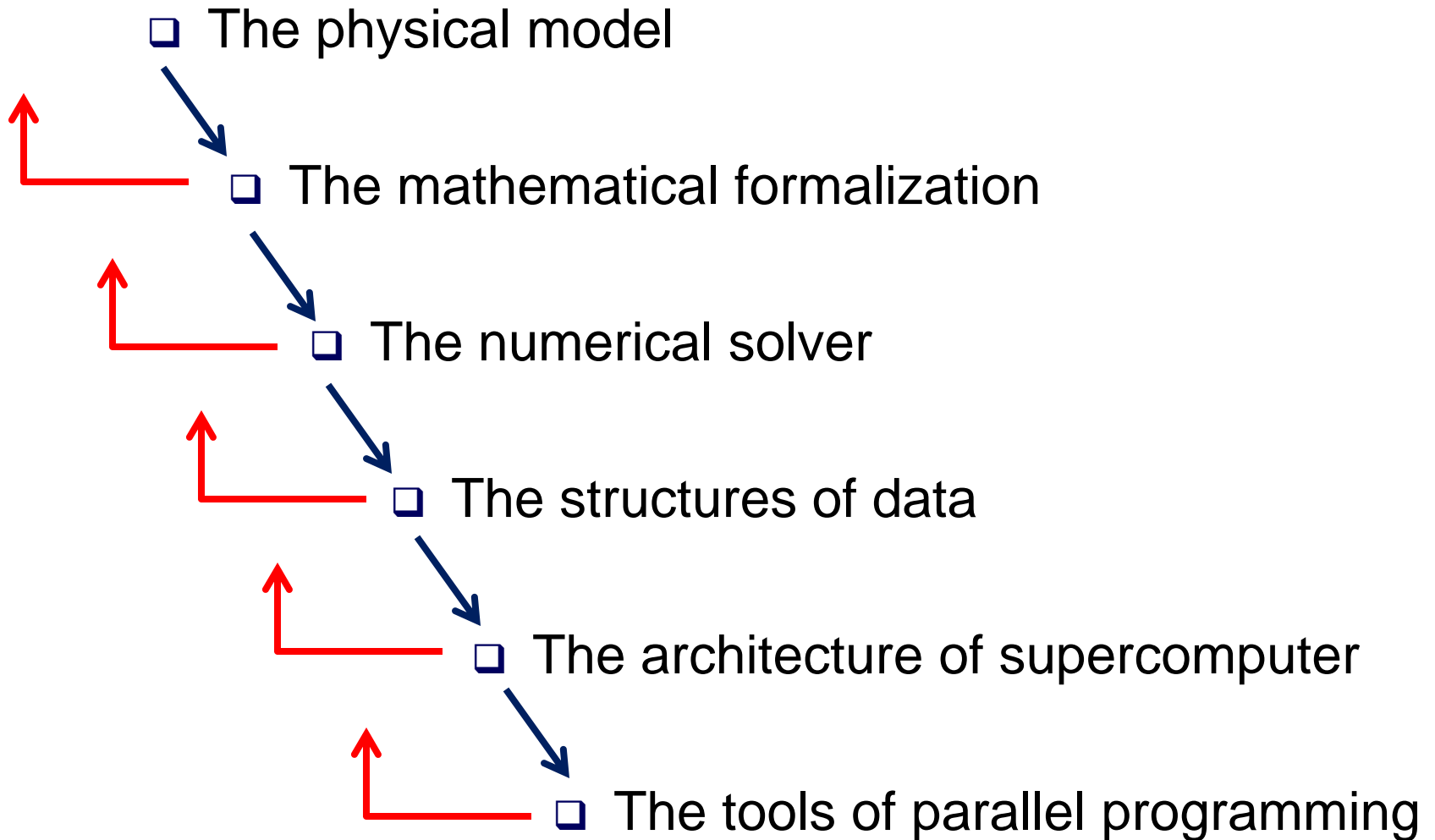
Rank	System	Cores	Rmax (TFlop/s)	Rpeak (TFlop/s)	Power (kW)
1	Sunway TaihuLight - Sunway MPP, Sunway SW26010 260C 1.45GHz, Sunway, NRCCPC National Supercomputing Center in Wuxi China	10,649,600	93,014.6	125,435.9	15,371
2	Tianhe-2 (MilkyWay-2) TH-IVB-FEP Cluster, Intel Xeon E5-2692 12C 2.00GHz, TH Express-2, Intel Xeon Phi 3151P, NUDT National Super Computer Center in Guangzhou China	3,120,000	33,862.7	54,902.4	17,808
3	Piz Daint - Cray XC50, Xeon E5-2690v3 12C 2.60GHz, Aries interconnect, NVIDIA Tesla P100, Cray Inc Swiss National Supercomputing Centre (CSCS) Switzerland	361,760	19,590.0	25,036.3	2,270
4	Gyokkou - ZettaScaler-2.2 HPC system, Xeon D-1501 12C 1.3GHz, Infiniband EDR, PEZY-SC2 700MHz, ExaScaler Japan Agency for Marine Earth Science and Technology Japan	19,860,000	19,135.8	28,192.0	1,350
5	Titan - Cray XK7, Opteron 6274 16C 2.00GHz, Cray Gemini interconnect, NVIDIA K20x, Cray Inc DOE/SC/Oak Ridge National Laboratory United States	560,640	17,590.0	27,112.5	8,209
6	Sequoia - BlueGene/L, PowerPC 16C 1.60 GHz, Custom, IBM DOE/NNSA/LLNL United States	1,572,864	17,173.2	20,132.7	7,890
7	Trinity - Cray XC40, Intel Xeon Phi 7250 68C 1.4GHz, Aries interconnect, Cray Inc. DOE/NNSA/ANL/SNL United States	979,968	14,137.3	43,902.6	3,844
8	Cori - Cray XC40, Intel Xeon Phi 7250 68C 1.4GHz, Aries interconnect, Cray Inc. DOE/SC/LBNL/NERSC United States	622,336	14,014.7	27,880.7	3,939
9	Oakforest-PACS - PRIMERGY CX1640 M1, Intel Xeon Phi 7250 68C 1.4GHz, Intel Omni-Path, Fujitsu Joint Center for Advanced High Performance Computing Japan	556,104	13,554.6	24,913.5	2,719
10	K computer, SPARC64 VIIIfx 2.0GHz, Tofu interconnect, Fujitsu RIKEN Advanced Institute for Computational Science (AICS) Japan	705,024	10,510.0	11,280.4	12,660

The hybrid supercomputers

The motivation – (iii) design concept



The motivation – (iii) **co-design** concept

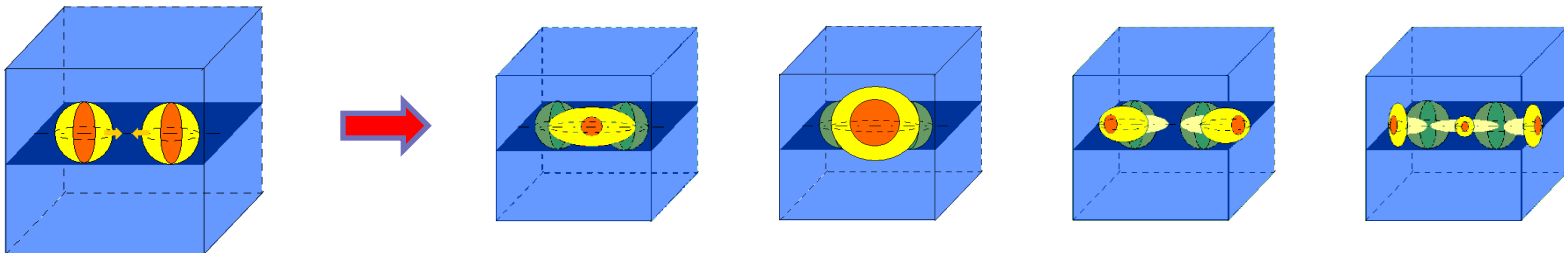
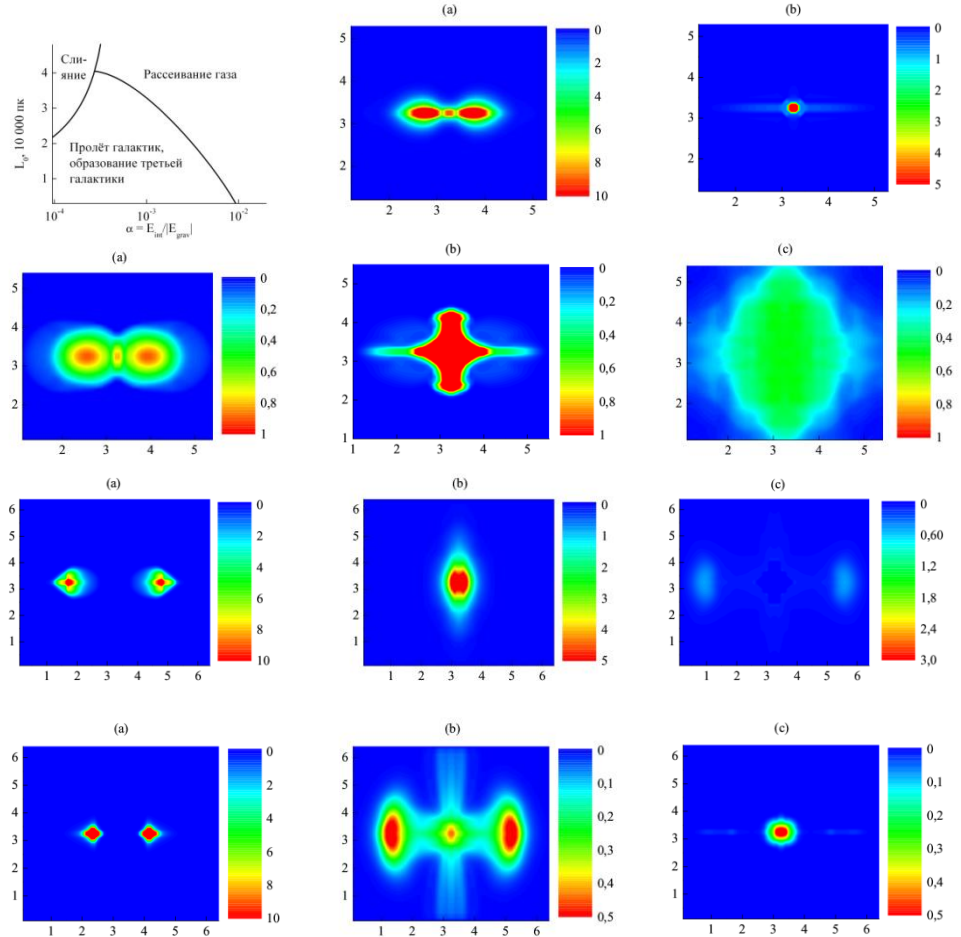


The hydrodynamics of interacting galaxies (2011)

In hydrodynamic model with analytical stellar component was shown four scenarios of central collision of two galaxies:

1. The coalescence
2. The dissipation of the gas components of the galaxies
3. The free expansion
4. The expansion with the formation of a new galaxy with no stellar component

1. Vshivkov, Lazareva, Snytnikov, Kulikov, Tutukov, ApJS, 2011
2. Tutukov, Lazareva, Kulikov, Astron Rep., 2011



The model of collisionless component

The disadvantages of N-body model

- a spurious generation of entropy
- a problem of choice of the kernel function in cell
- a necessary minimal number of particles in cell
- increased communication overhead
- poor load balancing
- a thermodynamically inconsistent of star formation

The hydrodynamic alternative

- The pressureless hydrodynamic
- The collisionless hydrodynamic*

The model of collisionless component

$$\frac{\partial f}{\partial t} + v_i \frac{\partial f}{\partial x_i} + a_i \frac{\partial f}{\partial v_i} = 0$$

$$d^3v = dv_x dv_y dv_z$$

$$\rho = \int m f d^3v$$

$$u = \rho^{-1} \int m f v d^3v$$

$$\sigma_{ij}^2 = \rho^{-1} \int m f (v_i - u_i)(v_j - u_j) d^3v = \sigma_{ji}^2$$

- It is important to movement of the cluster and not single particle
- No thermal transfer effects (*the property of almost all the astrophysical problems*)
- The velocity dispersion is much less than the velocity squared

$$\frac{\partial \rho}{\partial t} + \nabla \cdot (\rho u) = 0$$

$$\frac{\partial \rho u}{\partial t} + \nabla \cdot (\rho u u) = -\nabla (\rho \sigma^2) - \rho \nabla \Phi$$

$$\frac{\partial \rho E_{ij}}{\partial t} + \nabla \cdot (\rho E_{ij} u) = -\nabla \cdot (2\rho \sigma_{ij}^2 u) - 2(\rho u, \nabla \Phi)$$

$$\rho E_{ij} = \rho \sigma_{ij}^2 + \rho u_i u_j$$

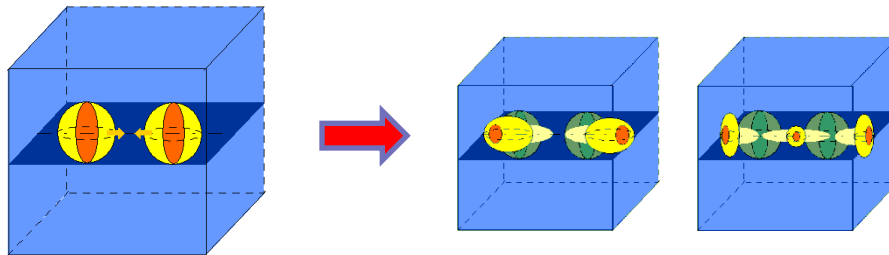
The model of collisionless component

The advantages of collisionless hydrodynamic

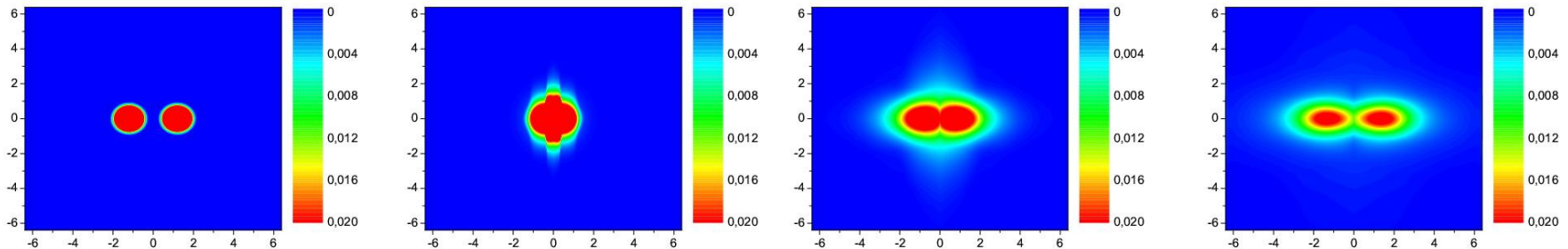
- a thermodynamically consistent of star formation
- one numerical method for gaseous and stellar components

The disadvantages of collisionless hydrodynamic

- The applicability of approach in each a specific problem



Kulikov, ApJS, 2014



The numerical methods

SPH approach

- Robustness of the algorithm
- Galilean-invariant solution
- Simplicity of implementation
- Flexible geometries of problems
- High accurate gravity solvers

- Artificial viscosity is parameterized
- Variations of the smoothing length
- The problem of shock wave and discontinuous solutions
- Instabilities suppressed
- The method is not scalable

AMR approach

- Approved numerical methods
- No artificial viscosity
- Higher order shock waves
- Resolution of discontinuities
- No suppression of instabilities
- Correct turbulence solution

- The complexity of implementation
- The effects of mesh
- Problem of the minimal mesh resolution
- Not Galilean-invariant solution
- The method is not scalable

The numerical methods

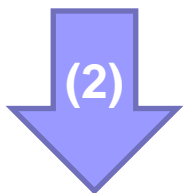
- ❑ The moving mesh approach (*AREPO, Springel, 2010*)
- ❑ The classic ALE-approach (*BETHE-Hydro, Murphy & Burrows, 2008*)
- ❑ The hybrid method on regular mesh (*Kulikov, 2004, from bachelor thesis*)

The main features of original methods

- ❑ The over definition hydrodynamic equations
- ❑ The operator-splitting approach
- ❑ The combination Godunov – Roe – PPML methods
- ❑ Using a regular mesh

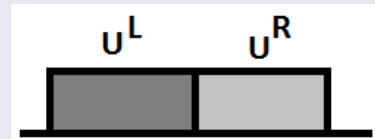
The numerical methods

$$\frac{\partial}{\partial t} \begin{pmatrix} \rho \\ \rho \vec{v} \\ \rho E \\ \rho \varepsilon \end{pmatrix} + \nabla \cdot \begin{pmatrix} \rho \cdot \vec{v} \\ \rho \vec{v} \cdot \vec{v} \\ \rho E \cdot \vec{v} \\ \rho \varepsilon \cdot \vec{v} \end{pmatrix} = \begin{pmatrix} 0 \\ -\nabla p \\ -\nabla \cdot (p \vec{v}) \\ -p \nabla \cdot (\vec{v}) \end{pmatrix} \quad (1) \quad \frac{\partial}{\partial t} \begin{pmatrix} \rho \\ \rho \vec{v} \\ \rho E \\ \rho \varepsilon \end{pmatrix} = \begin{pmatrix} 0 \\ -\nabla p \\ -\nabla \cdot (p \vec{v}) \\ -p \nabla \cdot (\vec{v}) \end{pmatrix}$$



$$\frac{\partial f}{\partial t} + \nabla \cdot (f \cdot \vec{v}) = 0$$

The Riemann problem



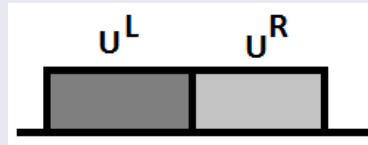
$$\frac{\partial u}{\partial t} + B \frac{\partial u}{\partial x} = 0 \quad B = R \Lambda L \quad LR = I$$

$$L \frac{\partial u}{\partial t} + LR \Lambda L \frac{\partial u}{\partial x} = 0 \quad w = Lu$$

$$\frac{\partial w}{\partial t} + \Lambda \frac{\partial w}{\partial x} = 0 \quad w(x, t) = w(x - \Lambda t) \quad u = Rw$$

The numerical methods – PPML approach

The Riemann problem

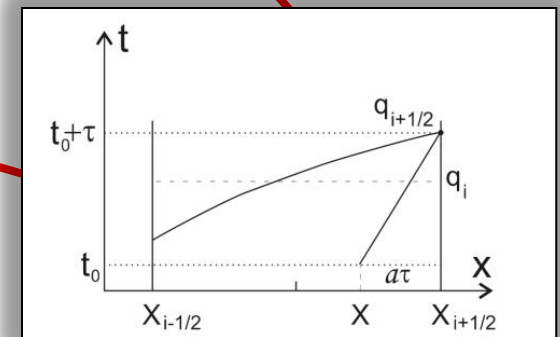


$$\frac{\partial u}{\partial t} + B \frac{\partial u}{\partial x} = 0 \quad B = R\Lambda L \quad LR = I$$

$$L \frac{\partial u}{\partial t} + LR\Lambda L \frac{\partial u}{\partial x} = 0 \quad w = Lu$$

$$\frac{\partial w}{\partial t} + \Lambda \frac{\partial w}{\partial x} = 0 \quad w(x, t) = w(x - \Lambda t) \quad u = Rw$$

The piecewise-parabolic functions



The numerical methods. The Roe solver

The Roe solver

$$[\rho] = \sqrt{\rho_L \rho_R}$$

$$H = \frac{p}{\rho} + \varepsilon$$

$$[H] = \frac{\sqrt{\rho_L} H_L + \sqrt{\rho_R} H_R}{\sqrt{\rho_L} + \sqrt{\rho_R}}$$

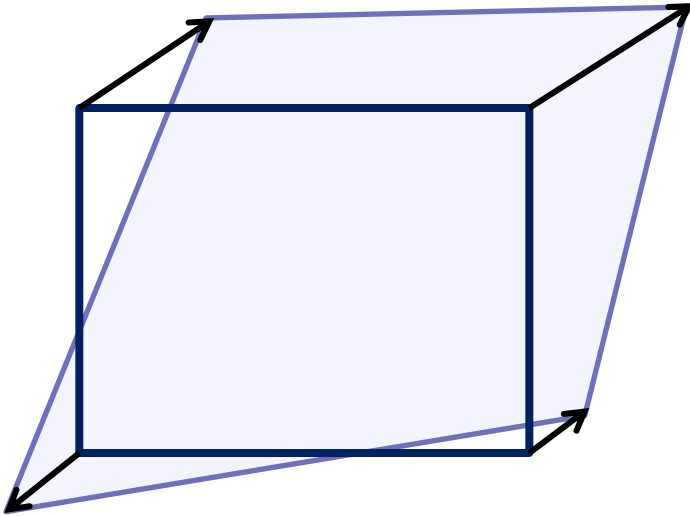
**The modification of
Roe solver**

$$[\rho] = \frac{\rho_L^{3/2} + \rho_R^{3/2}}{\sqrt{\rho_L} + \sqrt{\rho_R}}$$

$$[p] = \frac{\sqrt{\rho_L} p_L + \sqrt{\rho_R} p_R}{\sqrt{\rho_L} + \sqrt{\rho_R}}$$

**The reason – accurate
approximation of
boundary gas-vacuum**

The numerical methods. The advection transport



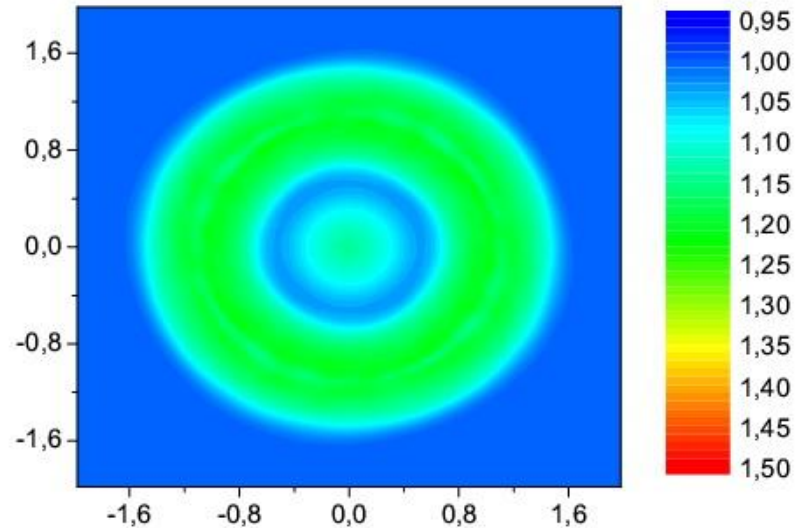
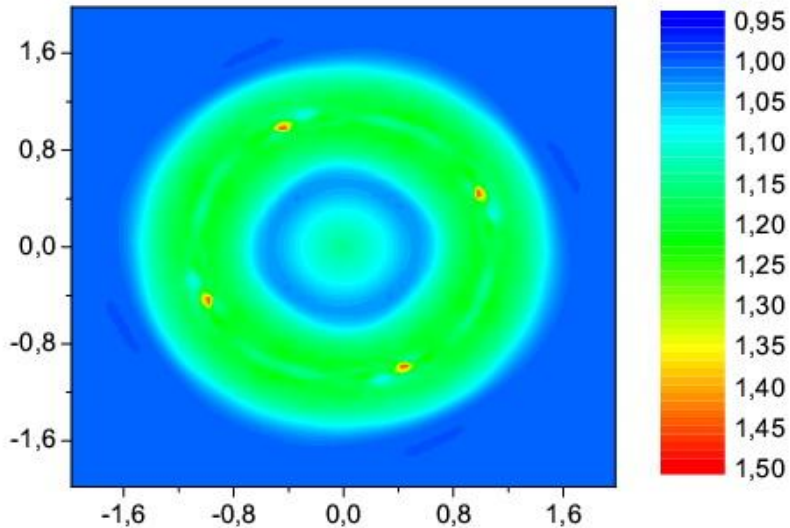
$$\frac{\partial z}{\partial t} + \nabla \cdot (z\vec{v}) = 0$$

$$[v] = \frac{\sqrt{z_L} v_L + \sqrt{z_R} v_R}{\sqrt{z_L} + \sqrt{z_R}}$$

1/16	2/16	1/16
2/16	4/16	2/16
1/16	2/16	1/16

$$F_{i+1/2,kl}^{n+1/2} = [v]_{i+1/2,k,l} \times \begin{cases} z_{ikl}, & [v]_{i+1/2,k,l} \geq 0 \\ z_{i+1,kl}, & [v]_{i+1/2,k,l} < 0 \end{cases}$$

The numerical methods. The advection transport



0	0	0
0	1	0
0	0	0

1/16	2/16	1/16
2/16	4/16	2/16
1/16	2/16	1/16

The over definition hydrodynamic equation

$$\rho E = \rho \varepsilon + \frac{\rho v^2}{2} \quad \begin{matrix} \nearrow \\ \searrow \end{matrix} \quad \begin{matrix} \|V\| = \sqrt{2(E - \varepsilon)} \\ \rho \varepsilon = \left(\rho E - \frac{\rho v^2}{2} \right) \end{matrix}$$

1. The renormalization of the velocity vector length, it's direction remaining the same (*on boundary gas-vacuum*)*.
2. The entropy (or internal energy) correction (*on regular density*)**

Such a modification of the method keeps the detailed energy balance and entropy nondecrease guarantee

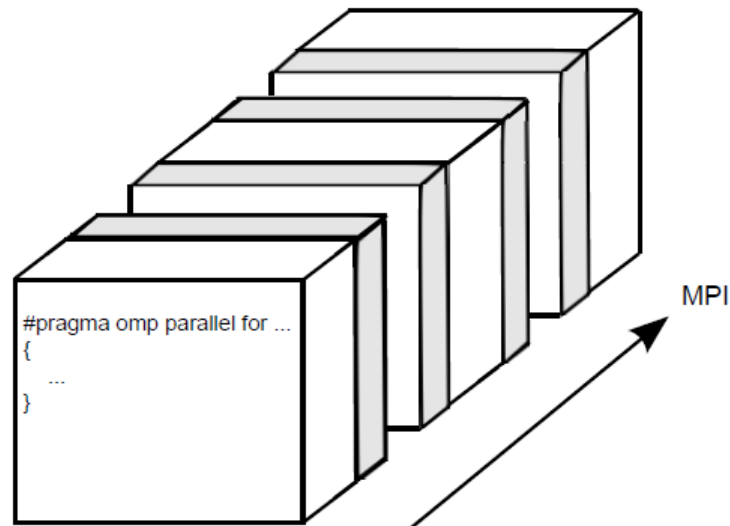
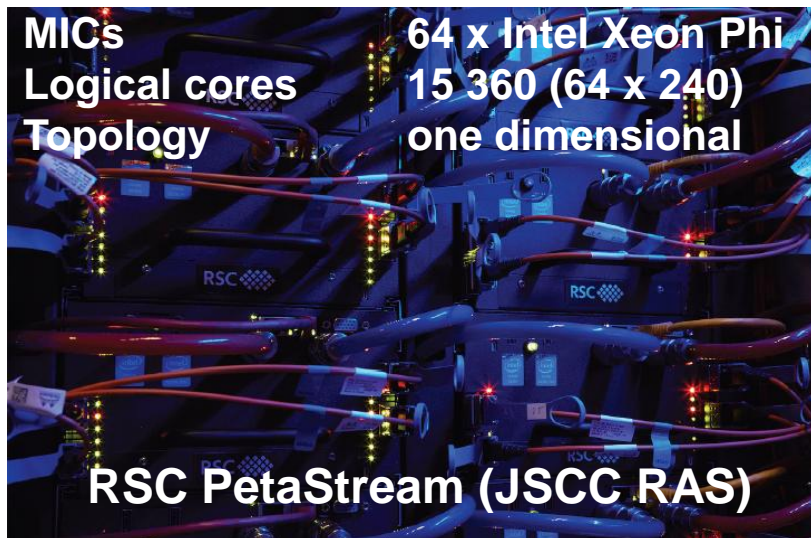
*) Vshivkov V., Lazareva G., Snytnikov A., Kulikov I., Tutukov A. Computational methods for ill-posed problems of gravitational gasdynamics // J. Inv. Ill-Posed Problems, 19. 2011, 151-166

**) Godunov S., Kulikov I. Computation of Discontinuous Solutions of Fluid Dynamics Equations with Entropy Nondecrease Guarantee // J. Comp. Math & Math. Phys., 54, 2014, 1012-1024

The verification of numerical method

- ❑ **One dimensional test for shock tube** (*discontinuous analytical solution*)
- ❑ **Test of Aksenov** (*continuous analytical solution*)
- ❑ **The Kelvin-Helmholtz instability**
- ❑ **The Releigh-Taylor instability**
- ❑ **The Sedov blast wave**
- ❑ **The control of angular momentum impulse test**
- ❑ **The expansion of gas into a vacuum**
- ❑ **The Evrard collapse**
- ❑ **The collapse of molecular cloud**
- ❑ **The fall of G2 onto Sgr A***
- ❑ ...

The parallel implementation



1. The speed-up factors of 134 on 260 logical cores
2. The efficiency of 92% on 64 MICs (or on 15 360 cores)
3. The 29 GFLOPS of scalar performance (or 40% from peak)

The simulation of behavior of parallel implementation on 983 040 cores by means **AGNES*** system the 80% efficiency was shown

*Podkorytov et al., LNCS 2010

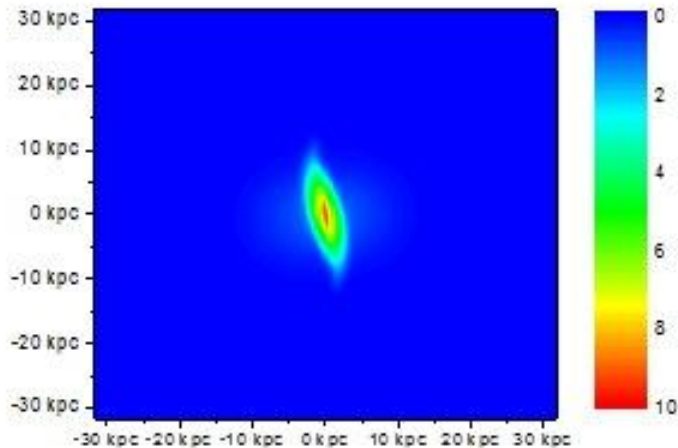
The numerical method. The summary

- ❑ The high-order (low-dissipation) numerical solution
- ❑ Not using of artificial viscosity or limiters
- ❑ The Galilean-invariant of numerical solution
- ❑ Entropy non-decrease guarantee
- ❑ Regular procedure for extension on other numerical models (*by example Boltzmann and MHD equations*)
- ❑ Simplicity of parallel implementation on hybrid and classic supercomputers
- ❑ Potential infinity scalability

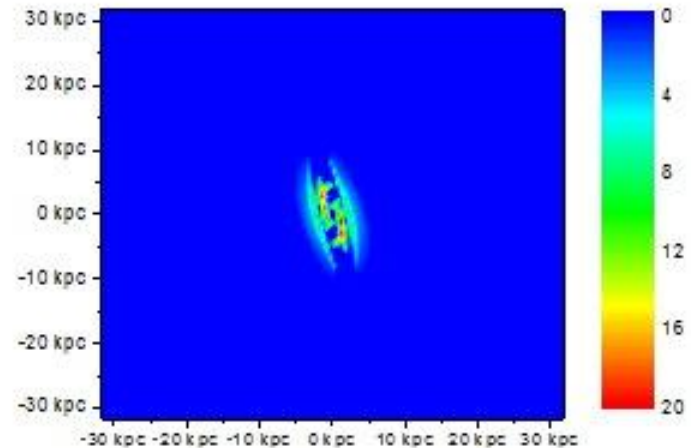
The interacting galaxies

The model:	two-phase model (hydrodynamic + Boltzmann)
The profiles:	self-gravitating rotational equilibrium*
The mass of galaxy:	$10^{13} M_{\odot}$
The subgrid physics:	star formation supernovae feedback H_2 formation cooling / heating

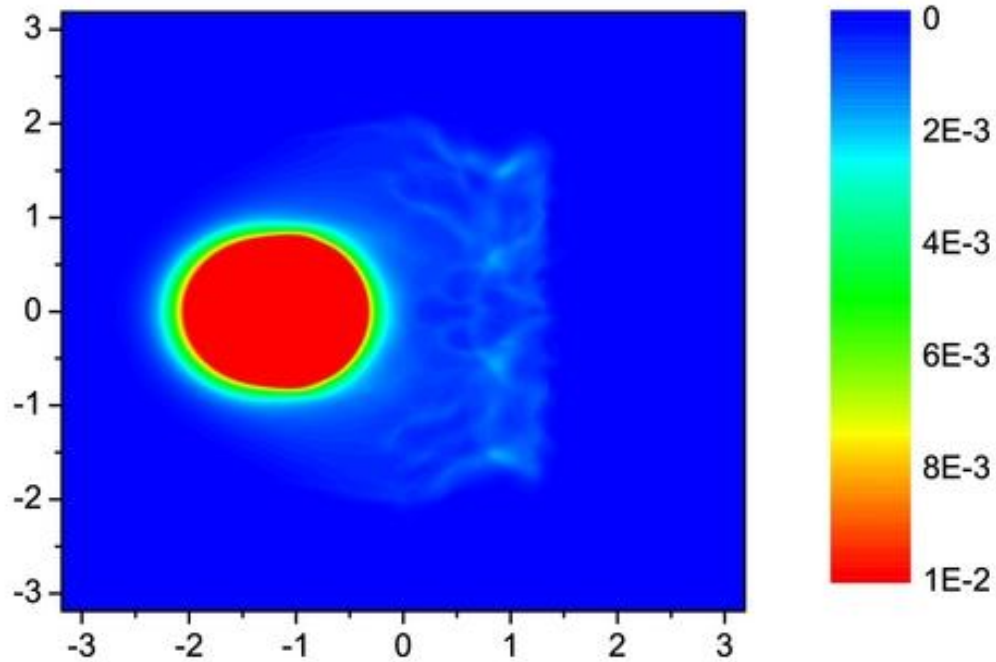
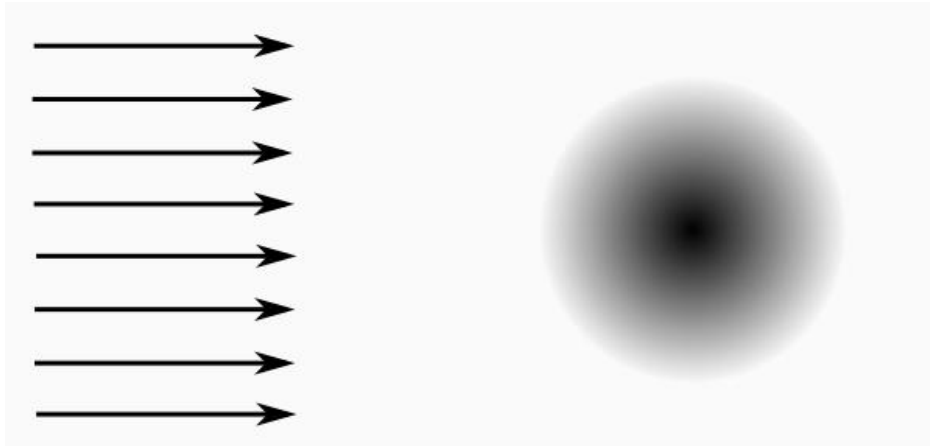
Molecular hydrogen



Star formation

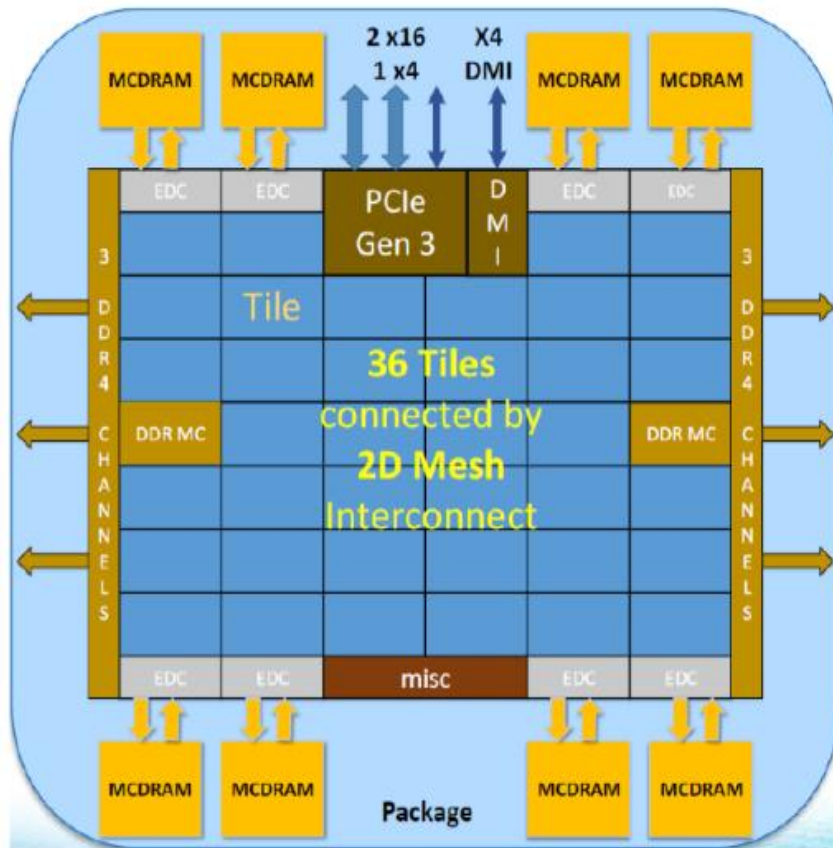


The Jellyfish galaxy



Where is TFLOPS+ on Intel Xeon Phi???

KNL Overview



TILE		
2 VPU	CHA	2 VPU
Core	1MB L2	Core

Chip: 36 Tiles interconnected by **2D Mesh**

Tile: 2 Cores + 2 VPU/core + 1 MB L2

Memory: MCDRAM: 16 GB on-package; High BW

DDR4: 6 channels @ 2400 up to 384 GB

IO: 36 lanes PCIe* Gen3. 4 lanes of DMI for chipset

Node: 1-Socket only

Fabric: Intel® Omni-Path Architecture on-package (not shown)

Vector Peak Perf: 3+TF DP and 6+TF SP Flops

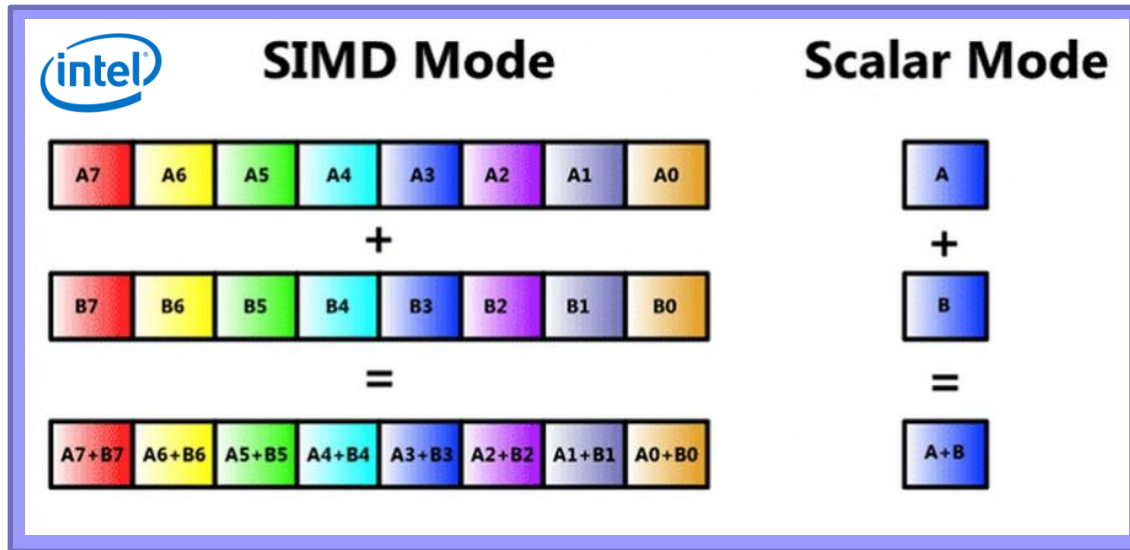
Scalar Perf: ~3x over Knights Corner

Streams Triad (GB/s): MCDRAM : 400+; DDR: 90+

MCDRAM
~5X Higher BW
than DDR

- Source Intel: All products, computer systems, dates and figures specified are preliminary based on current expectations, and are subject to change without notice. KNL data are preliminary based on current expectations and are subject to change without notice. 1Binary Compatible with Intel Xeon processors using Haswell Instruction Set (except TSX). 2Bandwidth numbers are based on STREAM-like memory access pattern when MCDRAM used as flat memory. Results have been estimated based on internal Intel analysis and are provided for informational purposes only. Any difference in system hardware or software design or configuration may affect actual performance. *Other names and brands may be claimed as the property of others.

SIMD technology (SSE, AVX 512, ...) + HLL solver



Vectors

$$\frac{\vec{u}_k^{n+1} - \vec{u}_k^n}{\tau} + \frac{F_{k+1/2} - F_{k-1/2}}{h_i} = q_k$$

$$F_{k+1/2}^{HLL} = \frac{\lambda_{k+1} F_k^n - \lambda_k F_{k+1}^n + \lambda_k \lambda_{k+1} (U_{k+1}^n - U_k^n)}{\lambda_{k+1} - \lambda_k}$$

Red arrows point from the terms in the first equation to the corresponding terms in the second equation: from \vec{u}_k^{n+1} to F_k^n , from \vec{u}_k^n to F_{k+1}^n , and from $F_{k+1/2} - F_{k-1/2}$ to $\lambda_k \lambda_{k+1} (U_{k+1}^n - U_k^n)$.

The intrinsic of AVX 512

<code>_mm512_set1_pd</code>	- set value for a vector
<code>_mm512_load_pd</code>	- load a vector from main memory
<code>_mm512_mul_pd</code>	- vector multiply
<code>_mm512_add_pd</code>	- vector summation
<code>_mm512_sub_pd</code>	- vector substitution
<code>_mm512_store_pd</code>	- store a vector to main memory

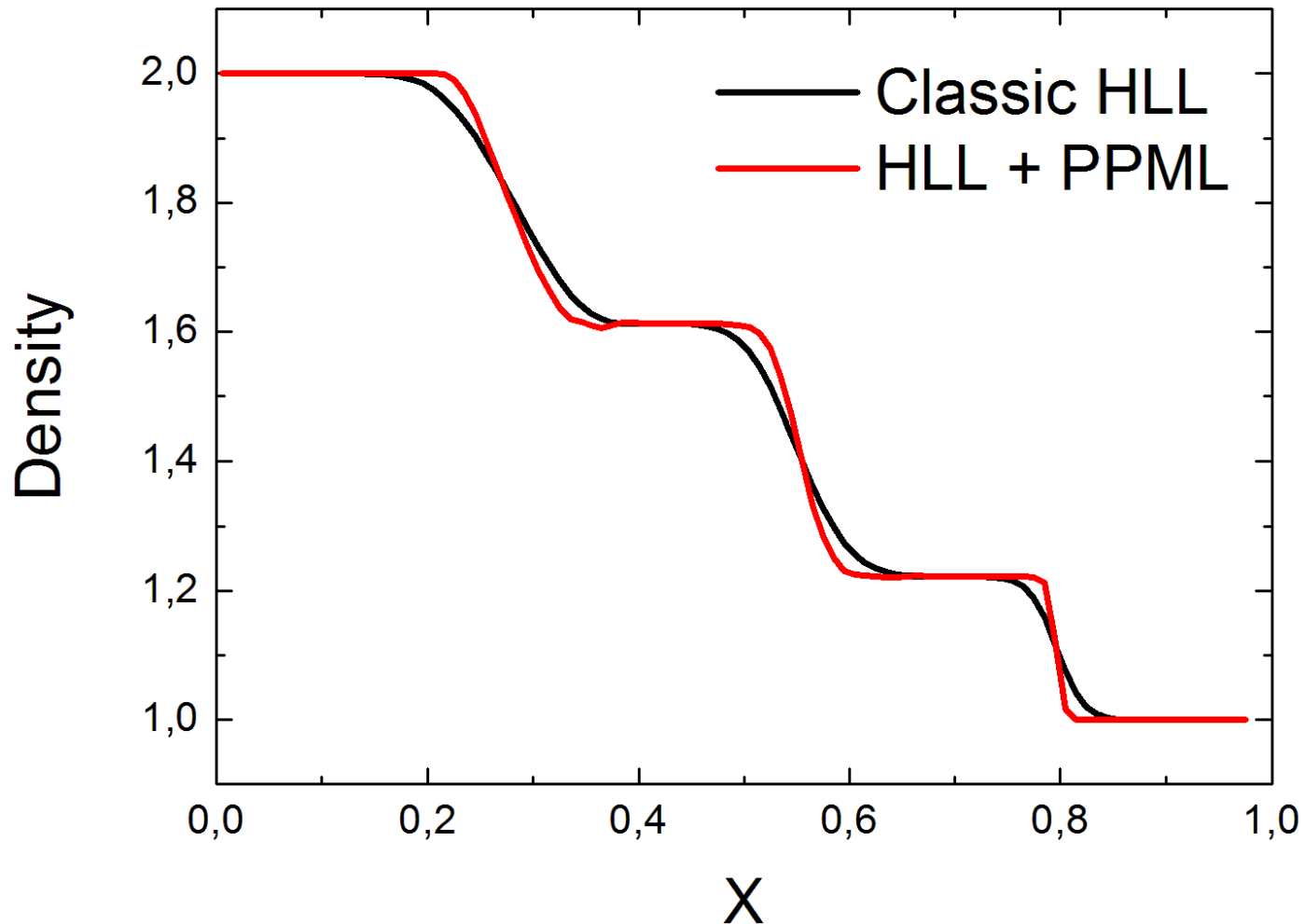
```
mpiicc -xMIC-AVX512 -qopenmp -O3 -o astroph.mic astroph.cpp -lm
```

Main advantages is 302 GFLOPS on Intel Xeon Phi

Main disadvantages – formation of the 8-double elements vector for computing

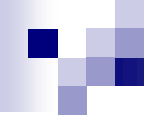
Pitfalls: associative of cache memory, align of memory, schedule distribution, data dependency

HLL? Where is high order and low dissipation?



The publications

- 1. Kulikov I. GPUPEGAS: A New GPU-accelerated Hydrodynamic Code for Numerical Simulations of Interacting Galaxies // The Astrophysical Journal Supplements Series. – 2014. – V. 214, 12. – P. 1-12**
- 2. Kulikov I.M., Chernykh I.G., Snytnikov A.V., Glinskiy B.M., Tutukov A.V. AstroPhi: A code for complex simulation of dynamics of astrophysical objects using hybrid supercomputers // Computer Physics Communications. – 2015. – V. 186. – P. 71-80**
- 3. Godunov S.K., Kulikov I.M. Computation of discontinuous solutions of fluid dynamics equations with entropy nondecrease guarantee // Computational Mathematics and Mathematical Physics. – 2014. – V. 54, № 6. – P. 1012-1024**
- 4. Kulikov I., Vorobyov E. Using the PPML approach for constructing a low-dissipation, operator-splitting scheme for numerical simulations of hydrodynamic flows // Journal of Computational Physics. – 2016. – V. 317. – P. 318-346.**



The sponsors

Grant of the President of Russian Federation

MK –1445.2017.9

Grants of Russian Foundation for Basic Research:

15-01-00508

**Thank you for your
attention!**